Supplementary Information:

Rubrene micro-crystals from solution routes: their crystallography, morphology and optical property

Liwei Huang, Qing Liao, Qiang Shi, Hongbing Fu, Jinshi Ma, and Jiannian Yao

State Key Laboratory for Structural Chemistry of Unstable and Stable Species,

Institute of Chemistry, Chinese Academy of Sciences, Beijing, 100190, P. R. China

E-mail: hongbing.fu@iccas.ac.cn; jnyao@iccas.ac.cn

(A)

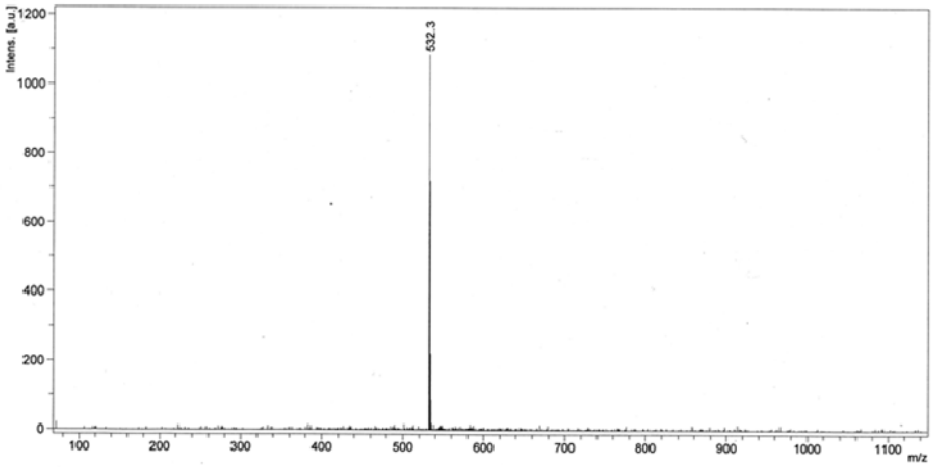

(B)

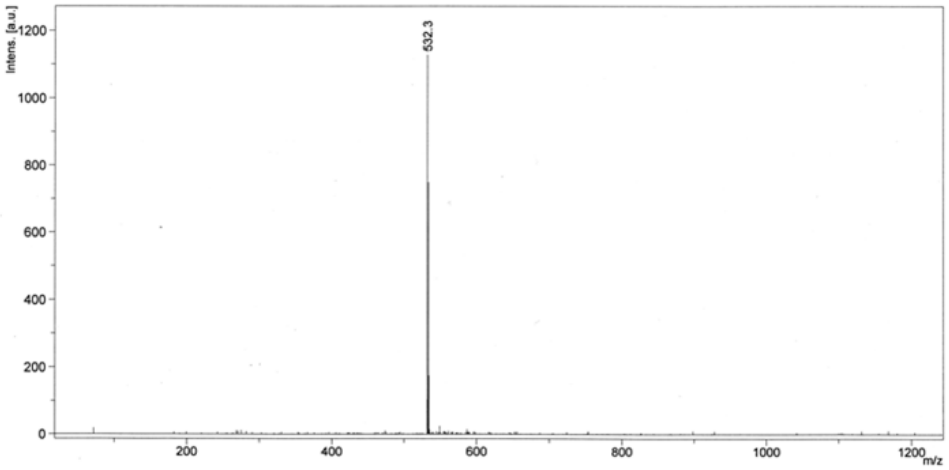

Figure S1. the MALDI-TOF mass spectra of (A) rubrene powders purchased from Aldrich, and (B) micro-crystals prepared by reprecipitation.

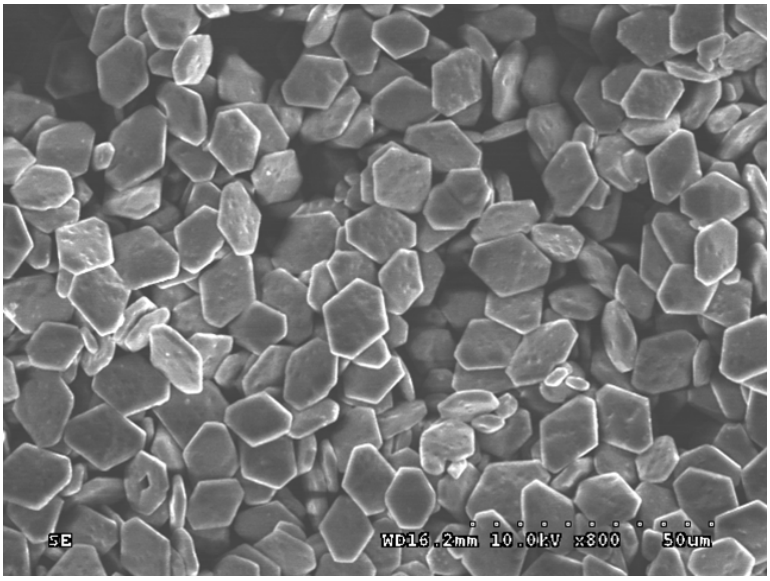

Figure S2. SEM images of truncated rhombic plates, which shows the immediate state from rhombus to hexagon.

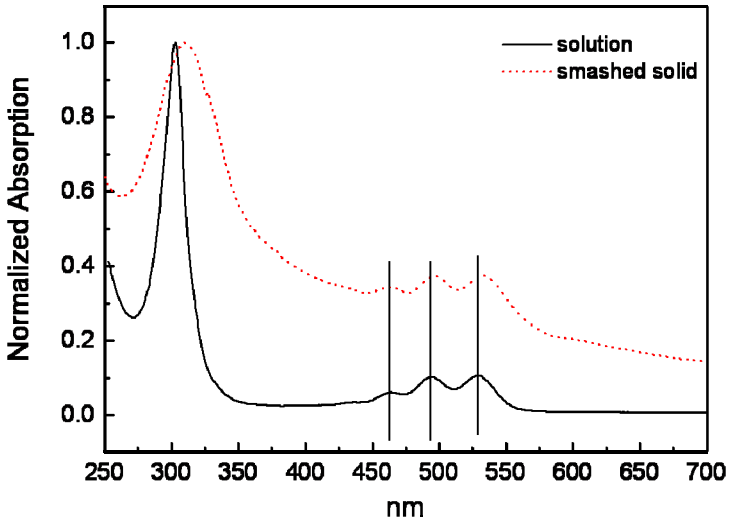

Figure S3. Normalized absorption spectra of rubrene solution in chloroform (black line) and smashed rubrene crystals (dashed line). The transmission spectra of rubrene MCs cannot be detected while directly deposited on the quartz substrates, in result of too strong reflection and absorption. But when MCs are smashed into smaller crystals, the absorption bands of solid on quartz substrates can be achieved

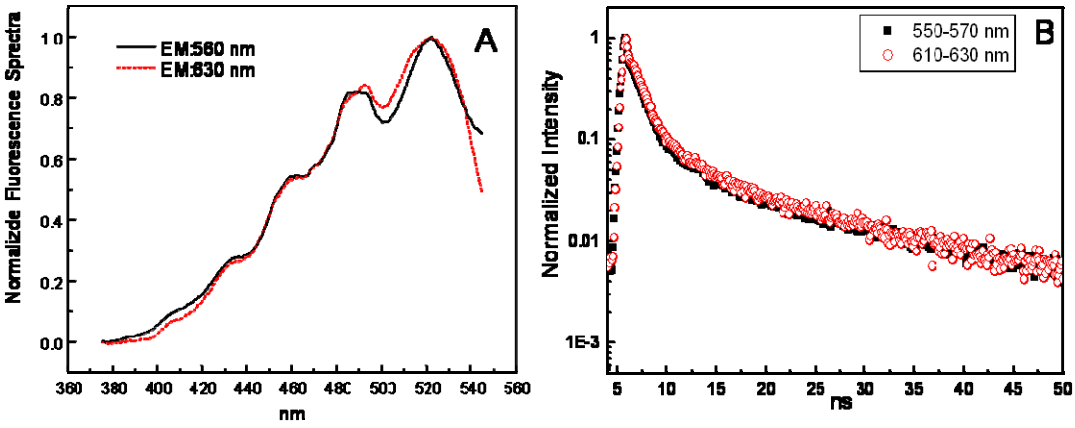

Figure S4. (A) Normalized fluorescence excitation spectra of rubrene hexagonal plates, at the emission of 560 nm (solid line) and 630 nm (dashed line). (B) Normalized fluorescence decay of rubrene hexagonal plates, gathered in 550-570nm (solid square) and 610-630 nm (hollow circle).

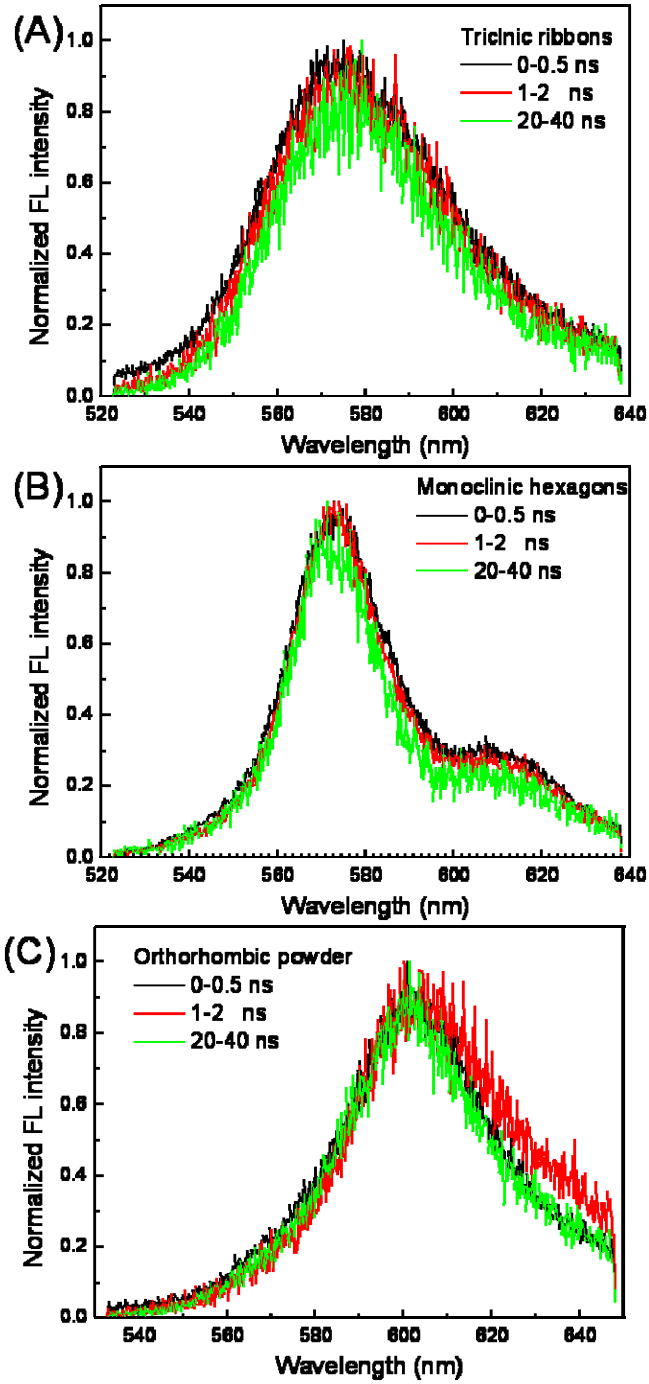

Figure S5. The spectral snapshots of different time range: 0~1 ns (black), 2~3 ns (red), 20~40 ns (green), for the samples of triclinic ribbons (A), monoclinic hexagonal plates (B) and orthorhombic powder (C).

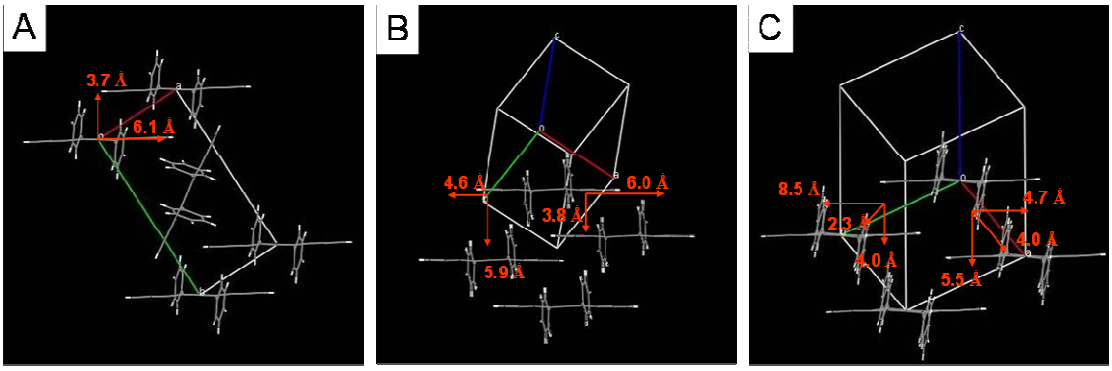

Figure S6. Illustration of the closet molecular packing plane in three crystal structures: (A) orthorhombic, (B) triclinic, and (C) monoclinic crystals, with the value of stacking distance, short-axis displacements, and long-axis displacement. For the triclinic crystals, the closet stacking distance of 3.8 Å, the long-axis displacement of 6.0 Å, and the absence of short-axis displacement, is very similar to the situation along the a-axis of orthorhombic crystals, along which cofacial π-stack interactions and electronic couplings are quiet efficient. For the monoclinic crystals, whether in any directions, the stacking distance is large, and the long-axis displacement is away from the extrema in the evolution of the transfer integrals. Moreover, the short-axis shows displacements of 2.3 Å or even 4.0 Å, so the overlapping of adjacent molecules will be very weak.

Table S1. Calculation results of lattice energy for triclinic and monoclinic crystals, performed by Materials Studio under the COMPASS force field.

	Lattice energy (kcal/mol)	Van der Waal contributaion (kcal/mol)	Electrostatic contribution (kcal/mol)	Molecular number per unit cell
Monoclinc unit cell	-107.883	-99.075	-8.808	2
Triclinic unit cell	-50.886	-50.055	-0.831	1